Growth of Cayley and diluted Cayley trees with two kinds of entities

N Vandewalle† and M Ausloos‡

SUPRAS, Institut de Physique B5, Université de Liège, Sart Tilman, B-4000 Liège, Belgium

Abstract. A kinetic growth model derived from the magnetic Eden model is introduced in order to simulate the growth of hierarchical structures, such as Cayley trees. We only consider the case where two kinds of entities are competing with each other and can be further subjected to an external field. The very relevant case in which both kinds of entities have different coordination numbers is introduced here for the first time, and is called the diluted Cayley tree. Physical and geometrical properties of the finite and infinite trees are exactly found and simulated. Finite-size effects are emphasized and illustrated on the global or local magnetization and on the chemical activity. Asymptotic limits are given in each case. The generated patterns can be related to a correlated percolation problem briefly discussed in the appendix.

1. Introduction

During the last decade, kinetic growth models have received much attention because of the natural forms and shapes that their non-equilibrium processes develop [1]. Thus, these models have possible applications in areas of science such as percolation [2], fracture [3] or crystal growth [4]. The most simple far from equilibrium growth model is that of Eden [5] which has led to several variants such as, for example, the 'Eden model A' [6]. In this model, the growth starts from a single particle called the 'seed' placed on an arbitrary lattice site. The growth process consists in selectively sticking a particle on an unoccupied lattice site in the immediate neighbourhood (the 'perimeter') of the cluster. This rule simulates, for example, the growth of bacteria cell colonies [5–7] and leads to compact clusters filling the Euclidian space. Variants of this simple rule were introduced to simulate, for example, sedimentation [8] or directed polymers [9]. Although the process is apparently simple, it is not yet fully understood [1–9].

Yet the Eden model and its present generalizations are too restrictive, because it is limited to the growth of a single species. However, natural systems can, by contrast, present different states. For example, biological entities like bacteria cells, for which the Eden model was constructed, can in fact present an extra degree of freedom, for example some gene of *salmonella* can be 'on' or 'off' [10].

Thus it is of interest to generalize the kinetic one-species growth models. In statistical physics, one simple way of representing a set of species is through a magnetic analogy, i.e. through a 'spin' taking a certain set of values. In previous works, we have added the notion of spin to the well known Eden [11] and DLA [12, 13] models. These 'generalized' or

† E-mail address: vandewal@gw.unipc.ulg.ac.be
‡ E-mail address: ausloos@gw.unipc.ulg.ac.be

'magnetic' kinetic growth models directly open many paths of investigation in (statistical) physics [11–13].

The aim of this paper is to present and solve such a magnetic-like growth on a Cayley tree (or Bethe lattice) and to discuss the physical and geometrical properties of the generated trees. Moreover, we will consider that both kinds of physical entities are geometrically different: both entities can, for example, have different but fixed branching coordination numbers. This 'condition' generates what we call *diluted Cayley trees*, apparently not examined up to now. From a more positive point of view, one can consider that the tree could evolve with multiple branching. This more general case of tree growth is discussed and is exactly solved here. Another generalization could consider a random value of the branching parameter at each growth step.

Such multi-species growths on hierarchical structures are not so marginal as might be thought at first: for example, bacteria cell colonies [10], dendrimers [14] and demographic problems [15] are addressed. The aim of this paper is not to pursue an exhaustive list of possible experimental relevant cases, but rather to develop statistical mechanics investigations on a new model and see whether interesting findings exist. The models presented here are clearly of theoretical interest because they can be connected to a correlated percolation which is a standard subject of investigation. A brief discussion of the correlated percolation problem on a Cayley tree is given in an appendix.

Furthermore, mathematical theory and formal examples of simple branching processes can be found in [15]. We will keep the 'magnetic picture and vocabulary' throughout the text because it is more traditional for Cayley trees.

In section 2, the Cayley tree model with fixed branching is presented and an exact solution is given for physical and geometrical quantities. These exact results are compared to simulation data. In section 3, we discuss the second model which generates diluted Cayley trees. Some conclusions are drawn in section 4. New interesting features are outlined, allowing for some thought as possible parameter control applications.

2. Growth of magnetic Cayley trees

2.1. The growth model

We recall first that a Cayley tree is a hierarchical lattice without loops with an asymptotically infinite dimension. Cayley trees are generated as follows. From a central site, z branches of unit length grow. The end of each branch is another growth site. At this step, a shell is formed by the z new sites; from each site of the first shell, $z - 1$ branches then grow out: the second shell is defined by the newly formed sites and this new shell contains $z(z - 1)$ sites. The process is then repeated. The parameter z is called the coordination number of the lattice. For $z = 2$, the tree reduces to a one-dimensional chain. Figure 1(*a*) shows three shells of a Cayley tree with a coordination number $z = 3$.

Consider now the growth of a Cayley tree when two possible Ising ($S = \frac{1}{2}$)-like types of entities can be deposited on the growth sites. Initially, a spin σ_0 (up or down) is dropped on the central site of the Cayley tree. It is the initiator of the growth and is also called the seed of the growth. Spins are then glued to each site of the first shell according to an *a priori* rule: the probabilities to glue an up-spin or to glue a down-spin are given by the Boltzmann factor $\exp(-\beta \Delta E)$ of the local gain of energy ΔE resulting from the addition of either type of spin. On each site, both probabilities are renormalized in the interval [0,1] over both up or down directions of the new spin. For each z-site of the first shell, a random number generator chooses a spin species with respect to the calculated probabilities. The
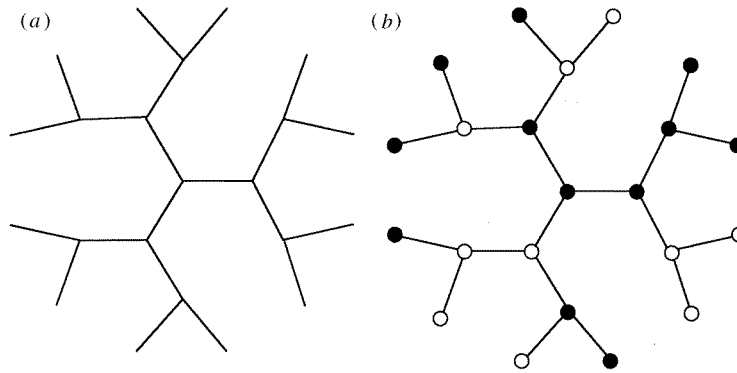
Figure 1. (*a*) Cayley tree of the third generation grown with $z = 3$. (*b*) Typical magnetic Cayley tree with $z = 3$ obtained by the model defined in section 2. Full and open circles represent up- and down-spins, respectively.

spins are frozen for ever and define a new spin-free perimeter, i.e. the set of empty sites in contact with the tree. This set forms the next shell, on which growth can take place in the same way. The process is repeated as many as g times.

The total energy E of a magnetic tree is obviously given by

$$E = -\frac{J}{2} \sum_{\langle i,j \rangle} \sigma_i \sigma_j - H \sum_i \sigma_i \qquad (2.1)$$

where the first summation occurs on the nearest-neighbour spins only. The first term describes a short-range interaction with coupling J between nearest-neighbour 'spins'. For a positive coupling, spins of the same species tend to aggregate in the tree while for a negative coupling, they tend to alternate. The second term in (2.1) defines a dimensionless field-like quantity for the orientation of the spins as if a 'magnetic field' is applied. The potential βH can indeed represent at first an external magnetic field, but can also be a chemical potential, a pressure field, etc. Although J and H are energies, the process is only of kinetic and geometric origin because the growth is driven by the probabilities $\exp(\beta J)$ and $\exp(\beta H)$, as we will see more explicitly below (section 2.2).

Such a process can be easily computed. Figure 1(*b*) shows a typical 'magnetic' Cayley tree with three shells, a tree which has grown from an up-spin as seed. Up- and down-spins are represented by full and open circles, respectively.

Here, at each generation, the growth occurs on all sites of the perimeter. Thus the kinetic growth model described above is an *isotropic* variant of the magnetic Eden model [11] which was built on a square lattice. Inclusion of a degree of freedom modelled by a spin permits one to study the distribution of 'spins' in the generated patterns, and therefore allows one to introduce physical quantities of interest, such as 'magnetization', and finally to merge a geometric model into a physical model and vice versa. Other physical quantities, such as correlation functions, susceptibility etc, are not studied here, but could receive some attention as well.

2.2. Physical and geometrical properties of the growing trees

At the gth generation of the tree, $z(z-1)^{g-1}$ spins are glued on the $(g-1)$th shell. The whole tree contains a 'mass' $S(g)$ of spins given by

$$S(g) = \frac{z(z-1)^g - 2}{z-2}. \tag{2.2}$$

The shell of the gth generation contains a number $N(g)$ of sites. For such trees, $N(g) = z(z-1)^{g-1}$ grows exponentially with g and is only dependent on z. $N(g)$ is also the number of paths that a self-avoiding random walker can follow to reach the external shell or the surface sites.

The tree may also be considered as a collection of $z(z-1)^{g-1}$ independent semi-open chains starting from the central site. The stochastic growth is similar to that used in the magnetic Eden model first studied on a square lattice [11]. For a one dimensional semi-open chain, it can be found that the probabilistic average $\overline{\sigma_g}$ of a spin at a distance g from the seed σ_0 is exactly given by

$$\overline{\sigma_g} = A\left(\frac{1 - B^g}{1 - B}\right) + \sigma_0 B^g \tag{2.3}$$

where the variables A and B are given by

$$A = \frac{\tanh(\beta J + \beta H) - \tanh(\beta J - \beta H)}{2} \tag{2.4a}$$

and

$$B = \frac{\tanh(\beta J + \beta H) + \tanh(\beta J - \beta H)}{2}. \tag{2.4b}$$

The magnetic (spin) analogy allows us to define physical quantities. The *global* 'magnetization' M of a tree of g shells is defined as the difference between the number of up- and down-spins normalized by the tree mass $S(g)$. The magnetization M is also the normalized summation of $\overline{\sigma_i}$ over all successive shells. M for a finite tree is given by

$$M = \frac{1}{S(g)}\left(\sigma_0 + \sum_{i=1}^{g} z(z-1)^{i-1}\overline{\sigma_i}\right). \tag{2.5}$$

Inserting equations (2.2) and (2.3) into equation (2.5), we obtain

$$M = \frac{(z-2)}{(z(z-1)^g - 2)}\left[\sigma_0 + \frac{zA}{1-B}\left(\frac{(z-1)^g - 1}{z-2}\right) + zB\left(\frac{1 - ((z-1)B)^g}{1 - (z-1)B}\right)\left(\sigma_0 - \frac{A}{1B}\right)\right]. \tag{2.6}$$

It is clear that this magnetization is not the equilibrium magnetization defined by the extremum of the free energy with respect to the field H. Here the magnetization does not minimize the free energy. The result of equation (2.6) holds for a non-equilibrium or 'quenched' system and is different from the mere annealed finite-size Ising case [16, 17].

In the presence of an external field, M tends asymptotically to $A/(1-B)$ independently of σ_0 and z. Figure 2 shows this asymptotic (for $g \to +\infty$) behaviour of M in the plane $(\beta J, \beta H)$. The magnetization M is asymptotically finite for $\beta H \neq 0$ and is only controlled by the sign of the field. Without the field ($\beta H = 0$), one should note that the asymptotic magnetization M tends to zero for all finite coupling values. One can notice an intermediate plateau around zero in the antiferromagnetic part of the $(\beta J, \beta H)$ plane of figure 2. In this region (i.e. for $\beta H < \beta J$), the antiferromagnetic coupling dominates the field and alternating configurations of spins are favoured, leading to a global zero magnetization for $g \to +\infty$.
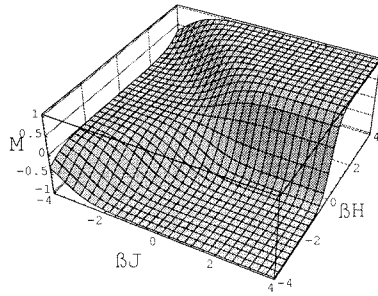
Figure 2. Asymptotic behaviour of the global magnetization of magnetic Cayley trees in the $(\beta J, \beta H)$ plane.

The *local* magnetization $\mu(g)$ of the gth shell is defined by the difference between the number N^+ of up- and the number N^- of down-spins in the gth shell normalized by the mass $z(z-1)^{g-1}$ of this shell. In the magnetic Cayley tree, $\mu(g) = \overline{\sigma_g}$ where $\overline{\sigma_g}$ is given by equation (2.3). It is worth pointing out that $\mu(g)$ tends asymptotically to $A/(1-B)$ (which is the quantity just discussed above) for finite βJ and βH values.

One should also remark that in kinetic growth models, when the geometry is intimately related to the physical growth process, interesting behaviours are generally found. This was the case, for example, of DLA or invasion percolation, in which fractal structures can be found [1, 13]. Here, the generated patterns are non-fractal by the definition of a tree (see section 2.1) but if we pay attention to the respective distribution of the spin species in the tree (see the appendix), filamentary clusters of spins are found for well-defined parameter $(\beta J, \beta H)$ values. This suggests that the internal structures of such trees are also interesting. The scope of this paper is, however, restricted to solving the global and surface spin composition of the trees.

2.3. Finite-size effect of trees grown in the presence of an external field

One is often interested in finite-size systems. Indeed, one should note that natural and physico-chemical systems have a finite size and only contain a few entities. Even though they are macroscopic systems, bacteria cell colonies contain no more than 10 000 cells [10]. Dendrimers, related macromolecules and nanocrystals are usually made of no more than ten generations or shells [14]. Therefore, it is useful to stress the size effect of the present growth model. This is done by comparing values for small trees (finite g) with the asymptotic values (figure 2).
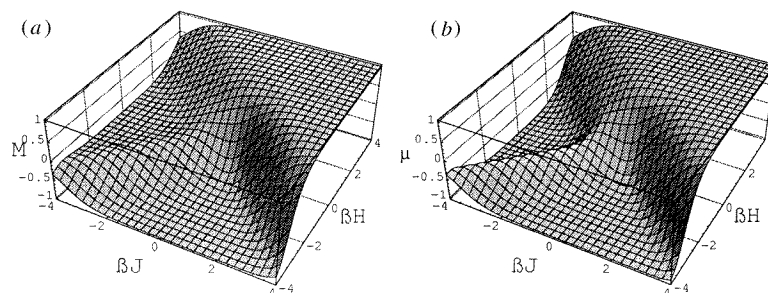

Figure 3. (*a*) Global magnetization M of small-size Cayley trees (fifth generation) with $z = 3$ grown from an up-spin as seed in the $(\beta J, \beta H)$ plane. (*b*) Surface magnetization $\mu(5)$ of the same trees.
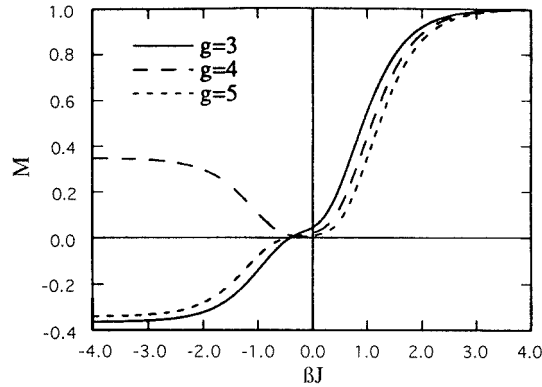
Figure 4. Global magnetization M as a function of βJ for Cayley trees ($z = 3$) grown without external field from an up-spin as seed. Different stages of the growth are shown ($g = 4, 5, 6$). One should note the varying sign of M with g at fixed coupling.

Figure 3(a) shows the magnetization M in the ($\beta J, \beta H$) plane of small trees ($z = 3, g = 5$) grown from an up-spin as seed. One should note that M is non-zero in the antiferromagnetic part of the diagram. In fact, introducing $z = 3$, $g = 5$ and $\beta J = -\infty$ into equation (2.6), we find that $M = -\frac{32}{94} \approx -0.3404$ for any βH value. Moreover, it should be stressed that (i) in this $\beta J < 0$ part of the diagram, M is a damped oscillating function of the size parameter g and converging towards zero (see equation (2.6)), and (ii) the amplitude of these oscillations is z-dependent. This damped oscillating behaviour is illustrated in figure 4 for the particular case $\beta H = 0$ (see the next subsection).

In the ferromagnetic part of the ($\beta J, \beta H$) plane, another finite-size effect is seen in the negative field region. It is essentially a *seed effect*. For a tree having grown from an up-spin, a strong coupling leads to all the spins being ordered in the same spin direction as that of the seed via nearest-neighbour interactions. When the field is dominated by the coupling, the sign of the global magnetization M is controlled by the seed sign, even though the field has a different sign.

Figure 3(b) shows the fifth shell local magnetization $\mu(5)$ of the same tree as those used for the global M magnetization shown in figure 3(a). Similar finite-size (oscillation and seed) effects occur *but are z-independent* as seen in equation (2.3). The spin composition of the external shell is thus strongly dependent on the initial seed *and* the generation g of the tree. In this sense, there are 'intrinsic finite-size effects'. Within this set of parameters, the global distribution of spin species is tunable. This opens new interesting prospects in various sciences.

2.4. Small trees grown in the absence of an external field

The variable A, defined in equation (2.2), characterizes the field effect: A reduces to zero without field and equation (2.6) then reduces to

$$M = \frac{(z - 2)\sigma_0}{(z(z - 1)^g - 2)}\left[1 + z\tanh(\beta J)\left(\frac{1 - ((z - 1)\tanh(\beta J))^g}{1 - (z - 1)\tanh(\beta J)}\right)\right]. \quad (2.7)$$

The zero-field case occurs when the growth process is controlled only by the local interactions.

Figure 4 shows the total magnetization M as a function of βJ for a finite Cayley tree ($z = 3$) grown without field from an up-spin as seed at different stages in its growth: $g = 3, 4$ and 5 (with mass $S = 22, 46$ and 766, respectively).

As similarly observed in the two-dimensional magnetic Eden model [18], the magnetization presents a smooth size-dependent 'transition' from 0 to 1 when the coupling $\beta J > 0$ is increased from 0 to a high value. As discussed in section 2.3, this transition is here also due to a *seed memory effect*. One should note (but it is not shown) that if the seed is 'down', M tends to -1 at large ferromagnetic coupling values because of the factor σ_0 appearing in equation (2.7). This means that above a sufficiently adequate (or 'critical') coupling value, the spin species of the seed itself dominates the other species. One can define the critical coupling value βJ_c as the inflexion point of the M curve by analogy with values derived from mean-field approximations in statistical mechanics. Taking the second derivative of equation (2.7) set to zero, one finds the value βJ_c, which diverges logarithmically with g. From equation (2.2), a variable change $g(S)$ leads to $\beta J_c \sim \ln(\ln(S))$. Thus, for large trees, a very large value of βJ is needed to obtain a non-zero magnetization for the system. This is in contrast to the behaviour observed in the MEM on the square lattice [18], where the critical value was found to grow logarithmically with the number of spins, i.e. $\beta J_c \sim \ln(S)$.

In the absence of an external field, the competition between the two species in the finite-size Cayley tree is thus strictly controlled by the seed σ_0 and the generation of the tree. Finally, notice that $g \gg 1$ and for large coupling values, $M(g)$ has the following behaviour:

$$M \sim \sigma_0 (\tanh(\beta J))^{g+1}. \tag{2.8}$$

For large positive coupling values, the dynamical behaviour of $M(g)$ is thus simply given by an exponential depending on the number g of generations. One should also note that the same exponential behaviour for $\mu(g)$ can be found from equation (2.2).

In the antiferromagnetic part ($\beta J < 0$), a slow oscillating convergence of $M(g)$ towards zero can also be seen. The discussion of the latter observation is identical to the one already made in section 2.3. The effect of the parity of g is also clearly seen here.

2.5. Simulations of Cayley trees

The global magnetization M of the resulting trees up to five shells grown *without field* and from an up-spin as seed is shown in figure 5. Each symbol represents the average of the magnetization over 100 simulated Cayley trees. Different coordination numbers have been used: $z = 3, 4$ and 5 for respectively square, triangle and circle symbols in figure 5. The full curves represent the theoretical curve given by equation (2.7). The global magnetization M of the simulated trees fits perfectly the theoretical curves.

3. Diluted Cayley trees

3.1. The growth model

In many cases, the examined species can have different 'coordination numbers' according to their state. Hence different coordination numbers z^+ and z^- for example, for a two state system, can be introduced. The total M should be strongly dependent on these parameters. Surprisingly, such an apparently simple tree model has not yet been studied to our knowledge. An example of multi-species growth is the evolution (catalysis) or
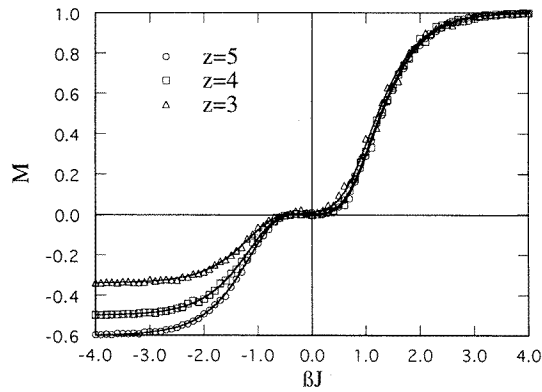
Figure 5. Global magnetization M of small Cayley trees ($g = 5$) grown from an up-spin as seed. Different coordination numbers are used. The measurements of M are averaged over 100 simulated trees; curves are theoretical values from equation (2.7).
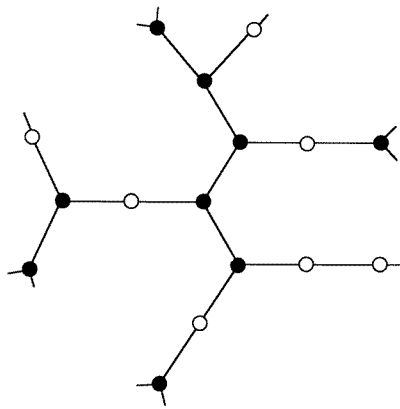

Figure 6. Typical magnetic diluted Cayley tree grown for $z^+ = 3$ and $z^- = 2$ up to the third generation. Full and open circles represent up- and down-spins, respectively.

reproduction (biological) processes where different filiation types can occur depending on the physical state of the entities.

The magnetic diluted Cayley tree model is introduced here for taking into account such a multi-species growth as an extension of the magnetic Cayley tree model (section 2). At each generation of the growth, from each up-spin, we assume that $(z^+ - 1)$ branches can grow out, while $(z^- - 1)$ branches can grow out from each down-spin. Figure 6 shows a typical magnetic diluted Cayley tree with three shells for $z^+ = 3$ and $z^- = 2$. The up- and down-spins are represented by full and open circles respectively. This tree has been grown from an up-spin.

Let us define some physical and geometrical quantities of interest for the magnetic Cayley tree. The gth shell contains a local mass $N(g)$ of sites dependent on the βJ and βH parameters, in obvious contrast to the magnetic Cayley tree model for which $N(g)$ was a constant for all values of the βJ and βH parameters. The branching ratio $b(g)$ of the

gth shell is defined by

$$b(g) = \frac{N(g+1)}{N(g)}. \tag{3.1}$$

One should note that it can take non-integer values, in contrast to the Cayley tree case where $b(g) = z - 1$ can take integer values only.

From the gth shell, $((z^+ - 1)N^+(g) + (z^- - 1)N - (g))$ bonds emerge. The so-called *chemical activity* $a(g)$ of the gth shell is defined as the normalized difference between bonds coming from up- and down-spins at a given g generation. The chemical activity of the gth shell is thus given by

$$a(g) = \frac{[(z^+ - 1)N^+(g) - (z^- - 1)N^-(g)]}{[(z^+ - 1)N^+(g) + (z^- - 1)N^-(g)]}. \tag{3.2}$$

One should note that for the magnetic Cayley tree case, the chemical activity $a(g)$ reduces simply to the *local magnetization* $\mu(g)$ of the gth shell.

3.2. Physical properties of diluted Cayley trees

Let us consider the behaviour of the local and global magnetization. This can be done by searching for the fixed point(s) of the growth process.

On a tree, each perimeter site of the growing g shell has only one single spin as nearest neighbour, a spin which is on the $(g - 1)$ shell. On each perimeter site, the probability to glue an up-spin is $(A + B + 1)/2$ if the neighbouring spin is up, and the gluing probability is $(A - B + 1)/2$ if the neighbouring spin is down. The probabilities to glue a down-spin are $(B - A + 1)/2$ and $(1 - A - B)/2$ for down and up neighbouring spins, respectively [11]. With this set of probabilities, it is easy to show that the local mass N on the average and the local magnetization μ on the average of two successive shells are related by the following recursive relations for the local mass:

$$N(g+1) = \frac{N(g)}{2}(z^+ + z^- - 2) + \frac{N(g)\mu(g)}{2}(z^+ - z^-) \tag{3.3}$$

and the non-normalized magnetization

$$N(g+1)\mu(g+1) = \frac{N(g)}{2}[(z^+ + z^- - 2)A + (z^+ - z^-)B]$$
$$+ \frac{N(g)\mu(g)}{2}[(z^+ + z^- - 2)B + (z^+ - z^-)A]. \tag{3.4}$$

Without field, equation (3.4) reduces to

$$\mu(g+1) = a(g)\tanh(\beta J). \tag{3.5}$$

For $z^+ = z^-$, the magnetic Cayley tree case must be recovered. Introducing $\mu(g+1) = \mu(g) = \mu_\infty$ into equation (3.4), the fixed point μ_∞ is simply found from a linear relationship and is given by $A/(1-B)$ corresponding to the asymptotical behaviour of the external shell local magnetization of the magnetic Cayley trees (see section 2.2).

However, for $z^+ \neq z^-$, introducing $\mu(g+1) = \mu(g) = \mu_\infty$ into equation (3.4), the latter becomes a quadratic equation in μ_∞ for which the roots are given by

$$\mu_\infty = \frac{1}{2(z^+ - z^-)}[(z^+ + z^- - 2)(B - 1) + (z^+ - z^-)A$$
$$\pm \{[(z^+ + z^- - 2)(B - 1) + (z^+ - z^-)A]^2$$
$$+ 4(z^+ - z^-)[(z^+ + z^- - 2)A + (z^+ - z^-)B]\}^{1/2}] \tag{3.6}$$
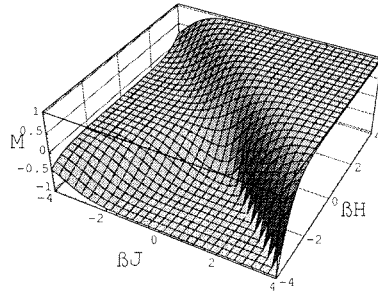
Figure 7. Global magnetization M in the $(\beta J, \beta H)$ plane of infinite magnetic diluted Cayley trees grown with $z^+ = 3$ and $z^- = 2$.

where the upper sign $(+)$ is only relevant for the $z^+ > z^-$ case and the lower sign $(-)$ only relevant for the $z^- > z^+$ case.

Thus the local magnetization $\mu(g)$ tends asymptotically (i.e. $g \to +\infty$) to be a constant μ_∞. This further leads to an asymptotic non-zero global magnetization M of the tree given by μ_∞.

Moreover, μ_∞ is independent of the seed sign. This means that *a spin species is asymptotically favoured even if the seed belongs to the other spin species*! Figure 7 shows the global magnetization $M = \mu_\infty$ in the $(\beta J, \beta H)$ plane of infinite diluted Cayley trees grown with $z^+ = 3$ and $z^- = 2$. The shape of μ_∞ is topologically similar to that of figure 2. However, M is markedly finite for all $\beta H = 0$ (except for $\beta J = 0$). It is remarkable that for the zero-field case, the magnetization is non-zero. This behaviour is markedly different from that found in the pure magnetic Cayley tree case.

Without field, equation (3.6) reduces to

$$\mu_\infty = \tfrac{1}{2}\left[\alpha(\tanh(\beta J) - 1) \pm \sqrt{\alpha^2(\tanh(\beta J) - 1)^2 + 4\tanh(\beta J)}\right] \qquad (3.7)$$

where α is a geometric quantity given by

$$\alpha = \frac{z^+ + z^- - 2}{z^+ - z^-}. \qquad (3.8)$$

Thus the local magnetization $\mu(g)$ tends to be asymptotically (i.e. $g \to +\infty$) a constant μ_∞. This leads to an asymptotic non-zero global magnetization M of the tree given by μ_∞. Even for the zero-field case, the magnetization is non-zero; this is quite different from the pure magnetic Cayley tree case.

Figure 8 shows the global magnetization M of infinite diluted Cayley trees grown without field and for different geometric factors α. The full and broken curves are drawn in figure 8 for positive and negative α values, respectively. This asymptotic behaviour of M is markedly different from the asymptotic case of the magnetic Cayley tree shown in figure 2.

3.3. Finite-size effects of diluted Cayley trees

As in section 2.3, finite-size systems are of interest. Figure 9 shows the global magnetization M (broken curves) of diluted Cayley trees grown without field and from two different seed species. The magnetization at generations 4 and 5 is shown. The bold full curve shows the asymptotic or fixed-point behaviour for these trees with $z^+ = 3$ and $z^- = 2$. The full and broken curves are theoretically obtained by iterating equation (3.4) for a positive and a negative seed, respectively. Large divergences from the fixed point are seen for large coupling values in the antiferromagnetic and ferromagnetic parts of the graph. For large
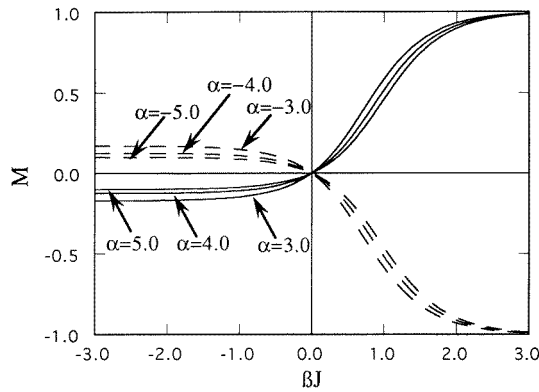
Figure 8. Global magnetization M as a function of $\beta J (\beta H = 0)$ of infinite magnetic Cayley trees grown with different α values.
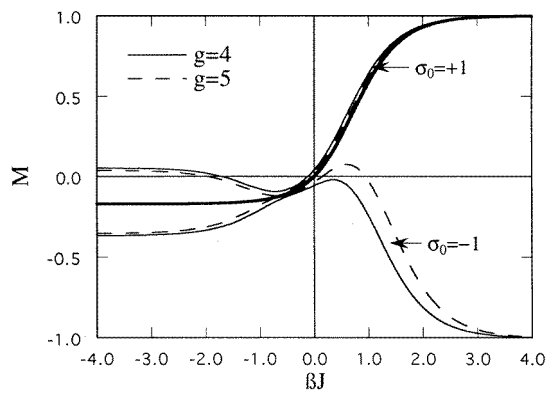

Figure 9. Global magnetization M as a function of βJ at two stages $g = 4$ and $g = 5$ of growth of magnetic diluted Cayley trees with $z^+ = 3$ and $z^- = 2$. Two different spin species are used as seed. The bold curve represents the fixed point locus μ_∞.

coupling values, we find a slow convergence of $\mu(g)$ towards μ_∞. This convergence is still slower when the sign of the seed is different from the sign of the growth-favoured species by the field. In such cases, the convergence of μ towards μ_∞ is difficult to observe because very large trees must be computed. In the case of $z^+ = 3$ and $z^- = 2$ (also shown in figure 9), antiferromagnetic coupling values lead to a slow oscillating convergence of the orbit of $\mu(g)$ around μ_∞. Thus, for small trees and antiferromagnetic coupling values, it is interesting to note that trees at two successive generations can exhibit rather different physical (M and μ) and geometrical (see also the branching ratio below) behaviour.

The chemical activity $a(g)$ and the branching $b(g)$ can be simply derived from $\mu(g)$ or equation (3.4). The asymptotic and the same finite-size behaviour shown in figure 9 are exhibited for $a(g)$ and $b(g)$ in figures 10 and 11, respectively. The bold curve is the asymptotic behaviour obtained from the combination of equations (3.1) and (3.2) with equation (3.7). One should note that the chemical activity is strongly seed- and shell-dependent for finite-size systems.

For diluted Cayley trees, geometrical quantities are also of interest because they are $(\beta J, \beta H)$-dependent. From equations (3.1) and (3.3), we can deduce that the asymptotic
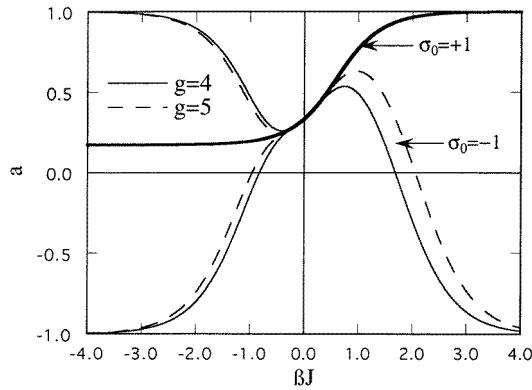
Figure 10. Chemical activity as a function of βJ at two stages $g = 4$ and $g = 5$ of growth of magnetic diluted Cayley trees with $z^+ = 3$ and $z^- = 2$. Two different spin species are used as seed. The bold curve represents the asymptotic behaviour derived from the fixed point locus μ_∞.
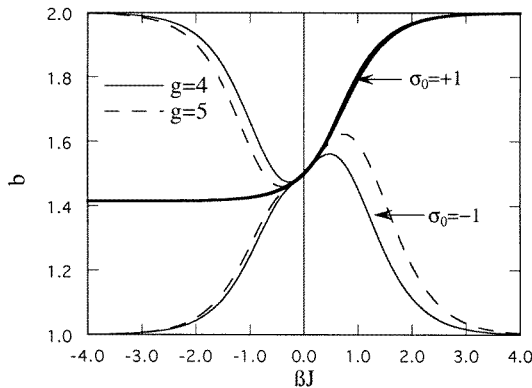

Figure 11. Branching ratio as a function of βJ at two stages $g = 4$ and $g = 5$ of growth for magnetic diluted Cayley trees with $z^+ = 3$ and $z^- = 2$. Two different spin species are used as seed. The bold curve represents the asymptotic behaviour derived from the fixed point locus μ_∞.

behaviour of the local mass $N(g)$ is exponential, i.e.

$$N(g, \beta J, \beta H) \sim \exp[b(g, \beta J, \beta H)g] \tag{3.9}$$

as expected for any hierarchical lattice (see section 2.1). Thus the total mass $S(g)$ of the diluted Cayley trees must also be βJ- and βH-dependent. Finite-size effects also influence the geometrical quantity N via the branching $b(g, \beta J, \beta H)$. Figure 12 presents the number of surface sites N on the average as a function of βJ of two small diluted trees of generation $g = 4$ and $g = 5$ grown without field βH. The seed was here fixed to be $+1$. The geometric parameters were fixed to be $z^+ = 3$ and $z^- = 2$. One can see that the number of surface sites is strongly βJ-dependent for a positive coupling.

One should note that for $\beta J = +\infty$, two trivial stable fixed points can be derived from equation (3.5), i.e. $\mu = -1$ and $\mu = +1$. The global magnetization of the tree has the same spin sign as the seed value. The generated lattice is simply a Cayley tree with the coordination number $z^{\text{sign}(\sigma_0)}$ of the seed species.
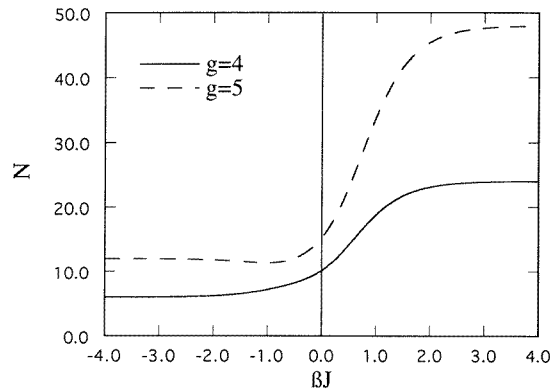
Figure 12. The averaged number of surface sites N as a function of βJ at two stages $g = 4$ and $g = 5$ of growth for magnetic diluted Cayley trees with $z^+ = 3$ and $z^- = 2$ grown from an up-spin as seed.

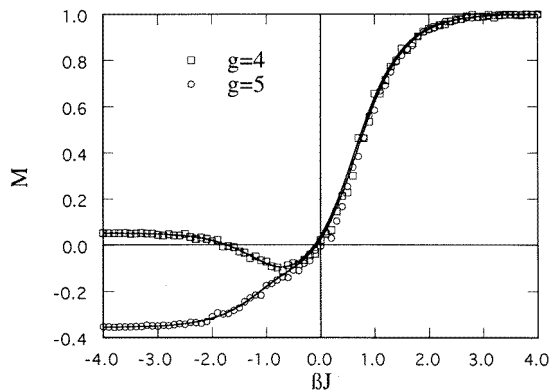**Figure 13.** Global magnetization M as a function of βJ for two growth stages $g = 4$ and $g = 5$ of *simulated* magnetic diluted Cayley trees with $z^+ = 3$ and $z^- = 2$ grown from an up-spin as seed. The full curves represent the theoretical curves.

3.4. Simulations of diluted Cayley trees

Numerical simulations agree with these predicted behaviours. The magnetization of small trees with $z^+ = 3$ and $z^- = 2$ grown without field is shown in figure 13. The full curve is the theoretical asymptotic magnetization or fixed point (equation (3.7)). Two stages of the growth ($g = 4$ and $g = 5$) are shown. The finite-size effects on the magnetization of figure 9 (see section 3.3) are clearly visible in figure 13.

4. Conclusion

The growth of hierarchical lattices or structures with two or even several kinds of entities is encountered in nature: polymers, epidemics, fragmentation, etc. The basic characteristic entities can be thought to be correlated via an internal coupling, and one entity could be favoured by an external field. At each generation, the growth can be thought to occur only on all sites of the perimeter or active shell. For such magnetically grown Cayley

trees, as introduced here, the growth is magnetically controlled only because the tree is forced to grow with a constant coordination number z. In the absence of a field, the global magnetization M of infinite trees is found to be zero for all finite coupling values. We have in particular found in section 2.4 that the kinetic behaviour of the local magnetization of the shells $\mu(g)$ decreases exponentially with the finite-size parameter g. Such kinetic behaviours are relevant for many natural or laboratory growth processes.

We have found in sections 2.3 and 2.4 that such intrinsic finite-size effects (i.e. the number of shell generations) strongly control the physical properties of the trees. Finite-size effects are likely to be relevant for studies of natural or artificial patterns.

A variant of the magnetic Cayley tree model called the magnetic diluted Cayley tree is also proposed in this paper; two kinds of coordination numbers *related to the states of the physical entities* are considered in a hierarchical lattice. Such cases seem very relevant in studies of polymers, catalytic or nuclear reaction dynamics, epidemics, etc.

Although the magnetic diluted Cayley tree model is a simple quenched model, it presents *new interesting features* from a statistical physics point of view. Both degrees of freedom (one geometric and one physical) are intimately related. The growing magnetic diluted Cayley tree *self-organizes* its geometry through the physical growth probabilities. The resulting asymptotic magnetization is seen to be generally non-zero and is independent of the seed sign. The finite-size effects are also strongly dependent of the various parameters.

The 'geometrical variables' (related to sites and bonds) $N(g)$, $b(g)$ as well as $S(g)$ and the 'physical variables' (related to spins) $M(g)$, $\mu(g)$ and $a(g)$ are strongly dependent on the *physical growth parameters βJ and βH* and the *geometrical parameters z^+, z^- and g*.

To put the results into proper perspective for our work, let us mention that the magnetic Cayley tree and the magnetic diluted Cayley tree can also serve as standard statistical mechanics models of phylogenetic tree evolution [19].

Further developments in these domains, besides more general coordination number z (random or not) distributions and more general spin states, should concern the statistical properties of the mass distribution of the spin-clusters in the growing trees, correlation effects and dynamic properties. Studying the present models by assimilating them to correlated percolation problems (see the appendix) can lead to some additional information of interest as well.

Appendix. Correlated percolation problems

In the bulk of the trees, it seems that the spins tend to aggregate in clusters. It is of interest to know the growth parameters for which a cluster of the same species spans the tree. If we consider the paths of the seed-type species from the initial site σ_0 to the extremities of the tree, we recover a correlated percolation problem [20]. One should note that the systems here are of the quenched type and differ from those studied in the majority of correlated (annealed) percolation problems. By studying the behaviour of the physical properties at the percolation threshold, we can get some additional information about the internal (spin) structure of the tree. Here, we limit our discussion to pure magnetic Cayley trees. The

percolation problem in magnetic diluted Cayley trees is much more complex and is outside the scope of this paper.

If we define the percolation threshold $(\beta J^*, \beta H^*)$ as the parameter values for which just a single cluster of the seed species spans the tree, the probability that a path of g spins grows from the seed to the surface multiplied by the number of branches of the tree $z(z-1)^{g-1}$ must be equal to unity. It is the condition that there exists just one percolating path. This gives

$$\beta J^* + \sigma_0 \beta H^* = \tfrac{1}{2} \ln[z^{1/g}(z-1)^{(g-1)/g} - 1] \tag{A.1}$$

for which the r.h.s. tends asymptotically $(g \to +\infty)$ to

$$\beta J^* + \sigma_0 \beta H^* = -\tfrac{1}{2} \ln(z-2). \tag{A.2}$$

In the absence of an external field and for a coordination number strictly greater than three $(z > 3)$, the coupling threshold βJ^* is always negative. This means that, even though the spins tend to alternate, one percolation path of σ_0 spins on the infinite lattice $(g \to +\infty)$ is possible. The percolation threshold corresponds to the uncorrelated $(\beta J^* = 0)$ case for a coordination number $z = 3$. Moreover, it was shown in section 2 that in the absence of an external field, M tends asymptotically to zero for all finite coupling values. Thus, the magnetization M is zero at the threshold for all $z > 2$. This means that the mass of the spanning or percolating cluster (of magnetization σ_0) is much smaller than the mass of the tree (for $\beta H = 0$). It is like a *filamentary percolation*. It would be interesting to observe the blocking of such a percolation and the distribution of substructures just as they are examined in the screening of species in phylogenetic tree growths [21].

However, in the presence of an external field, the magnetization (equation (2.6)) is asymptotically non-zero at the threshold and is dependent on the seed sign. The mass of the spanning cluster here is not negligible in front of the mass of the tree. In this case, the notion of filamentary percolation can only be used if M has the opposite sign to that of the seed, i.e. when the field has an opposite sign to that of the seed. Otherwise, it would be necessary to calculate the magnetization on the backbone, a calculation which is outside of the scope of this paper.

References

[1] Hermann H J 1986 *Phys. Rep.* **136** 153
[2] Bunde A, Hermann H J, Margolina A and Stanley H E 1985 *Phys. Rev. Lett.* **55** 653
[3] Ausloos M and Kowalski J M 1992 *Phys. Rev.* B **45** 12830
[4] Xiao R F, Alexander J I D and Rosenberger F 1988 *Phys. Rev.* A **38** 2447
[5] Eden M 1958 *Symp. on Information Theory in Biology* ed H P Yockey (New York: Pergamon) p 359
[6] Jullien R and Botet R 1985 *J. Phys. A: Math. Gen.* **18** 2279
[7] Barker G C and Grimson M J 1994 *J. Phys. A: Math. Gen.* **27** 653
[8] Meakin P 1993 *Phys. Rep.* **235** 189
[9] Kim J M 1993 *J. Phys. A: Math. Gen.* **26** L33
[10] Silverman M and Simon M 1983 *Mobile Genetic Elements* ed J A Shapiro (Orlando, FL: Academic) p 537
[11] Ausloos M, Vandewalle N and Cloots R 1993 *Europhys. Lett.* **24** 629; 1995 *J. Magn. Magn. Mater.* **140** 2185
    Ausloos M and Vandewalle N 1996 *Acta Phys. Pol.* B **27** 737
[12] Vandewalle N and Ausloos M 1994 *Diffusion Processes: Experiment, Theory, Simulations (Lecture Notes in Physics 438)* ed A Pekalski (Berlin: Springer) pp 283–94
[13] Vandewalle N and Ausloos M 1995 *Phys. Rev.* E **51** 597
[14] Tomalia D A, Naylor A M and Goddard W A 1990 *Angew. Chem. Int. Ed. Engl.* **29** 138–75
[15] Harris T E 1963 *The Theory of Branching Processes* (Berlin: Springer)
[16] Thompson C J 1972 *Mathematical Statistical Mechanics* (New York: McMillan) p 116
[17] Eggarter T P 1974 *Phys. Rev.* B **9** 2989

[18] Vandewalle N and Ausloos M 1994 *Phys. Rev.* E **50** R635
[19] Vandewalle N and Ausloos M 1995 *J. Physique* **5** 1011
[20] Wollman D A, Dubson M A and Zhu Q 1993 *Phys. Rev.* B **48** 3713
[21] Vandewalle N and Ausloos M 1996 *Physica* **90D** 262